

Laser Modification of Preformed Polymer Microchannels: Application To Reduce Band Broadening around Turns Subject to Electrokinetic Flow

Timothy J. Johnson,^{*,†} David Ross,[‡] Michael Gaitan,[§] and Laurie E. Locascio^{*,†}

Analytical Chemistry Division, Process Measurements Division, and Semiconductor Electronics Division, National Institute of Standards and Technology, 100 Bureau Drive, Stop 8394, Gaithersburg, Maryland 20899-8394

A pulsed UV excimer laser (KrF, 248 nm) was used to modify the surface charge on the side wall of hot-embossed microchannels fabricated in a poly(methyl methacrylate) substrate. Subablation level fluences, less than 2385 mJ/cm², were used to prevent any changes in the physical morphology of the surface. It is shown that the electroosmotic mobility, induced by an electric field applied along the length of the channel, increases by an average of 4% in the regions that have been exposed to UV laser pulses compared to nonexposed regions. Furthermore, application of UV modification to electroosmotic flow around a 90° turn results in a decrease in band broadening, as measured by the average decrease in the plate height of 40% compared to flow around a nonmodified turn. The ability to modify the surface charge on specific surfaces within a preformed plastic microchannel allows for fine control, adjustment, and modulation of the electroosmotic flow without using wall coatings or changing the geometry of the channel to achieve the desired flow profile.

The field of microfluidics is predicated on the concept of reducing laboratory-bench analytical chemistry instruments to miniature systems that are interconnected with micrometer-scale channels. To date, the majority of the devices reported in the literature, as well as those that are commercially available, have been fabricated using silica-based materials.^{1–3} However, polymeric materials are increasingly being used in microfluidic systems primarily because they offer the possibility of easy and inexpensive fabrication.^{4–8}

With silica-based or polymeric devices, fluid transport within the microchannels can often be achieved using electrokinetic,^{3,9–11} thermal,^{12,13} or mechanical pumping.¹⁴ Electrokinetic pumping has been the most common method for fluid transport due to its simplicity and because sample dispersion within the channel is minimal compared to dispersion induced by nonelectrically driven flow.^{15,16} Electrokinetic flow results when an electric field that is applied along the length of the channel interacts with the charged ions in the electric double layer near charged surfaces. The interaction forces the mobile ions in the double layer to exhibit a net migration, which leads to drag-induced bulk fluid flow.

Since the induced fluid motion is a wall-driven phenomenon, differences in the surface chemistry and surface charge from channel to channel, or spatially within a single microchannel, can have dramatic effects on the flow profiles, flow rates, and separations that occur within devices that utilize electrokinetics.^{4,6,15} Because of this variability, or the desire to controllably enhance or suppress the wall charge, researchers have developed techniques for rendering a uniform surface charge. For electroosmotic applications in silica and glass, covalent,^{17,18} noncovalent,¹⁹

[†] Analytical Chemistry Division.

[‡] Process Measurements Division.

[§] Semiconductor Electronics Division.

- (1) Harrison, D. J.; Manz, A.; Fan, Z. H.; Ludi, H.; Widmer, H. M. *Anal. Chem.* **1992**, *64*, 1926–1932.
- (2) Woolley, A. T.; Mathies, R. A. *Proc. Natl. Acad. Sci. U.S.A.* **1994**, *91*, 11348–11352.
- (3) Jacobson, S. C.; Hergenroder, R.; Koutny, L. B.; Ramsey, J. M. *Anal. Chem.* **1994**, *66*, 2369–2373.
- (4) Roberts, M. A.; Rossier, J. S.; Bercier, P.; Girault, H. *Anal. Chem.* **1997**, *69*, 2035–2042.
- (5) Martynova, L.; Locascio, L. E.; Gaitan, M.; Kramer, G. W.; Christensen, R. G.; Maccreehan, W. A. *Anal. Chem.* **1997**, *69*, 4783–4789.

- (6) Locascio, L. E.; Perso, C. E.; Lee, C. S. *J. Chromatogr., A* **1999**, *857*, 275–284.
- (7) Xu, J. D.; Locascio, L.; Gaitan, M.; Lee, C. S. *Anal. Chem.* **2000**, *72*, 1930–1933.
- (8) McCormick, R. M.; Nelson, R. J.; Alonsoamigo, M. G.; Benvegna, J.; Hooper, H. H. *Anal. Chem.* **1997**, *69*, 2626–2630.
- (9) Seiler, K.; Harrison, D. J.; Manz, A. *Anal. Chem.* **1993**, *65*, 1481–1488.
- (10) Koutny, L. B.; Schmalzing, D.; Taylor, T. A.; Fuchs, M. *Anal. Chem.* **1996**, *68*, 18–22.
- (11) Huang, X. C.; Quesada, M. A.; Mathies, R. A. *Anal. Chem.* **1992**, *64*, 967–972.
- (12) Jun, T. K.; Kim, C.-J. *Technol. Dig. Solid State Sensor Actuator Workshop* **1996**, 144–147.
- (13) Burns, M. A.; Mastrangelo, C. H.; Sammarco, T. S.; Man, F. P.; Webster, J. R.; Johnson, B. N.; Foerster, B.; Jones, D.; Fields, Y.; Kaiser, A. R.; Burke, D. T. *Proc. Natl. Acad. Sci. U.S.A.* **1996**, *93*, 5556–5561.
- (14) Wilding, P.; Pfahler, J.; Bau, H. H.; Zemel, J. N.; Kricka, L. J. *Clin. Chem.* **1994**, *40* (1), 43–47.
- (15) Ross, D.; Johnson, T. J.; Locascio, L. E. *Anal. Chem.* **2001**, *73*, 2509–2515.
- (16) Paul, P. H.; Garguilo, M. G.; Rakestraw, D. J. *Anal. Chem.* **1998**, *70*, 2459–67.
- (17) Culbertson, C. T.; Ramsey, R. S.; Ramsey, J. M. *Anal. Chem.* **2000**, *72*, 2285–2291.
- (18) He, H.; Li, H.; Mohr, G.; Kovacs, B.; Werner, T.; Wolbeis, O. *Anal. Chem.* **1993**, *65*, 123–127.
- (19) Pinto, D. M.; Ning, Y.; Figeys, D. *Electrophoresis* **2000**, *21*, 181–190.

and dynamic²⁰ wall coatings have been used. Similarly, dynamic coatings,^{21,22} polyelectrolyte multilayers,^{23,24} and surface chemical modifications²⁵ are beginning to be used in polymer microchannels.

In this paper, we report the use of an alternative approach for chemically modifying imprinted microchannels in polymer substrates. We will describe a method that uses a UV excimer laser to locally alter the chemistry and charge of a surface within a previously formed microchannel in poly(methyl methacrylate) (PMMA), but without ablating or changing the physical dimensions of the preformed channel. Previous researchers have documented that the surface properties (hydrophobicity, chemical functionality, surface charge) of laser ablated surfaces are altered compared to the surfaces of the native material or of microchannels formed by other techniques.^{4,6,26,27} Recently, it was reported that changes in the surface properties were not limited to ablation level laser pulses but that there is a measurable change in the polymer's surface chemistry, which results in an increased surface charge when exposed to UV pulses below the ablation threshold.²⁸ It is this subablation regime, combined with the spatial resolution of the excimer laser, that is utilized in this paper to modify local electrokinetic flow profiles within preformed microchannels.

A specific application of this surface modification technique is to reduce the band-broadening effects that occur due to electrokinetic flow around turns. It has been well documented that an analyte band will become distorted, or skewed, as it travels around a turn due to differences in the path length and differences in the magnitude of the electric field between the inside and the outside of the turn.^{29–31} Recently, many researchers have been attempting to develop microchannel turns that minimize band broadening by changing the microchannel geometry, i.e., the radius of curvature or the channel width.^{32–35} While these channel designs are successful, they often incorporate a decrease in channel width at the turn, which can lead to a dramatic increase in the electric field and Joule heating. As an alternative to altering the channel geometry, we propose to increase the surface charge on the outside wall of the turn to compensate for the decreased electric

field and increased path length. In this paper, we demonstrate the use of localized surface modifications by UV exposure to reduce dispersion in electrokinetic flow around turns. To our knowledge, this is the first report in the open literature that describes the combined use of laser patterning within preformed microchannels to locally affect and modulate flow.

EXPERIMENTAL SECTION

Reagents and Materials. Fluorescein bis(5-carboxymethoxy-2-nitrobenzyl) ether dipotassium salt (CMNB-caged fluorescein dye), 1-ethyl-3-(3-dimethylaminopropyl)carbodiimide hydrochloride (EDAC), and 5-(aminoacetamido) fluorescein were used as supplied by Molecular Probes (Eugene, OR). All buffer solutions were made using deionized water from a Millipore Milli-Q system (Bedford, MA). Caged dye solutions were prepared by dissolving ~1 mg of CMNB-caged fluorescein solid in 500 μ L of 20 mM (The accepted SI unit of concentration, mol/L, has been represented by the symbol M in order to conform to the conventions of this journal.), pH 9.4 carbonate buffer and were filtered before use with syringe filters (pore size 0.8 μ m). The EDAC and aminofluorescein were dissolved in 100 mM, pH 7 phosphate buffer to make a solution with a final concentration of 0.5 mM EDAC and 0.5 mM aminofluorescein.

Microchannels were made using UV-transparent PMMA sheet (Acrylite OP-4, Cyro Industries, Mt. Arlington, NJ). The glass transition temperature of PMMA is typically in the range of 100–120 °C. PMMA was chosen as the substrate material because it has a low absorption cross section at 248 nm (the wavelength of the excimer laser) and therefore allows us to more easily investigate subablation modification of the polymer's surface. Furthermore, it was necessary that the material be transparent to 337-nm light in order to perform the flow monitoring studies by the uncaging method. Nonetheless, because of the range of available light sources, the results of this study are not limited to PMMA.

Hot Imprinting Method. Prior to imprinting, the PMMA substrate was cleaned with compressed air. Channels were imprinted in the substrate material using a silicon stamp with a trapezoidal-shaped raised straight or 90°-turn channel.⁵ The PMMA was placed over the silicon stamp, the two items were placed between two aluminum heating blocks, and the temperature was raised to 110 °C. The assembly was then placed in a hydraulic press, and a pressure of 5.1 MPa (740 psi) was applied for 1 h. The imprinted substrate was then removed from the template and allowed to cool to room temperature. Channel dimensions were measured by optical profilometry.

Laser Modification Method. A 248-nm excimer laser system (LMT-4000, Potomac Photonics, Inc., Lanham, MD) was used to surface-modify the PMMA at fluences below the ablation threshold. The laser ablation threshold is defined for this study as the minimal fluence level where there is noticeable mass loss or morphological change to the surface of the PMMA substrate as observed from SEM images. The excimer laser system²⁸ contains a laser light source, a round aperture (592- μ m diameter) for delimiting the size and shape of the beam, a focusing lens (10 \times compound), a visible light source, a CCD camera to image the ablation process, and a controllable X–Y stage with a vacuum chuck to hold the substrate in place. The size-delimiting aperture

- (20) Chiem, N.; Harrison, D. J. *Anal. Chem.* **1997**, *69*, 373–378.
(21) Liu, Y.; Fanguy, J. C.; Bledsoe, J. M.; Henry, C. S. *Anal. Chem.* **2000**, *72*, 5939–5944.
(22) Wang, S.-C.; Perso, C. E.; Morris, M. D. *Anal. Chem.* **2000**, *72*, 1704–1706.
(23) Barker, S. L. R.; Ross, D.; Tarlov, M. J.; Gaitan, M.; Locascio, L. E. *Anal. Chem.* **2000**, *72*, 5925–5929.
(24) Barker, S. L. R.; Tarlov, M. J.; Canavan, H.; Hickman, J. J.; Locascio, L. E. *Anal. Chem.* **2000**, *72*, 4899–4903.
(25) Henry, A. C.; Tutt, T. J.; Galloway, M.; Davidson, Y. Y.; McWhorter, C. S.; Soper, S. A.; McCarley, R. L. *Anal. Chem.* **2000**, *72*, 5331–5337.
(26) Srinivasan, R.; Braren, B. *Chem. Rev.* **1989**, *89*, 1303–1316.
(27) Schwarz, A.; Rossier, J. S.; Roulet, E.; Mermod, N.; Roberts, M. A.; Girault, H. H. *Langmuir* **1998**, *14*, 5526–5531.
(28) Johnson, T. J.; Waddell, E.; Kramer, G. W.; Locascio, L. E. *Appl. Surf. Sci.*, in press.
(29) Jacobson, S. C.; Hergenroder, R.; Koutny, L. B.; Warmack, R. J.; Ramsey, J. M. *Anal. Chem.* **1994**, *66*, 1107–1113.
(30) Jacobson, S. C.; Ramsey, J. M. *Electrophoresis* **1995**, *16*, 481–486.
(31) Culbertson, C. T.; Jacobson, S. C.; Ramsey, J. M. *Anal. Chem.* **1998**, *70*, 3781–3789.
(32) Paegel, B. M.; Hutt, L. D.; Simpson, P. C.; Mathies, R. A. *Anal. Chem.* **2000**, *72*, 3030–3037.
(33) Culbertson, C. T.; Jacobson, S. C.; Ramsey, J. M. *Anal. Chem.* **2000**, *72*, 5814–5819.
(34) Molho, J. I.; Herr, A. E.; Mosier, B. P.; Santiago, J. G.; Kenny, T. W.; Brennen, R. A.; Gordon, G. B.; Mohammadi, B. *Anal. Chem.* **2001**, *73*, 1350–1360.
(35) Zubrisky, E. *Anal. Chem.* **2000**, 687A–690A.

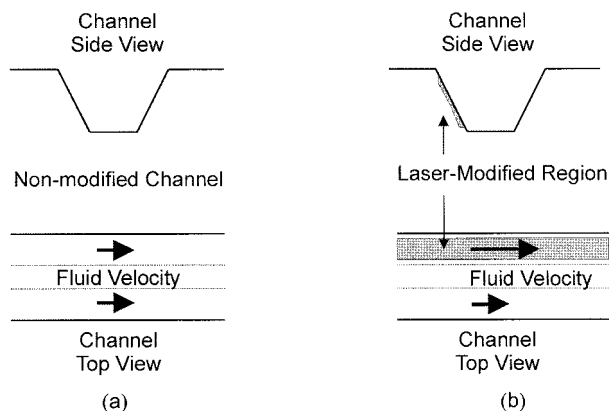


Figure 1. Schematic of the side and top views, and the corresponding electroosmotic flow profiles, of (a) a nonmodified and (b) a UV-modified, hot-imprinted microchannel. (b) Depicts the surface that was UV modified.

was chosen such that there would be minimal UV exposure to surfaces other than the channel's side wall. Also, a gas nozzle was present to sweep nitrogen over the substrate during processing, and a vacuum nozzle was located on the opposite side of the stage to remove debris. For the experiments conducted here, the X–Y stage was moved linearly at a rate of 1 mm/s, exposing the PMMA over the length of the channel such that the light exposed only one surface within the preformed channel, as shown in Figure 1. For the experiments in a straight channel, one side wall was modified over the entire length of the channel, whereas for the channel with a 90° turn, only a length of 500 μm of the outer wall on one arm of the turn was modified. The average power level per pulse was set to 2.58 μJ , $\sigma = 0.10 \mu\text{J}$ for the experiments in a straight channel and 4.50 μJ , $\sigma = 0.16 \mu\text{J}$ for the experiments in a 90°-turn channel. The average power per pulse, and corresponding standard deviation, were determined by three measurements of 100 pulses with an Energy Max 400 laser energy meter from Moletron Detector, Inc. (Portland, OR). The frequency of pulses was set to 200 Hz, with a constant pulse width of 7 ns. The light after being focused exposed a circular area of $1.90 \times 10^{-6} \text{ cm}^2$.

Fluorescent Labeling of Surface Carboxylate Groups.

Fluorescent labeling of the surface was used to image the charge density. The protocol used for labeling the surface carboxylate groups within the microchannels was a modification of a previously reported procedure.³⁶ The substrate with the uncovered microchannel (without the 'lid') was immersed in the EDAC/aminofluorescein solution for 15 h followed by an agitated rinse with 100 mM phosphate buffer, pH 7, then 138 mM carbonate buffer, pH 9.5, and then a final agitated rinse with the phosphate buffer. The channels were then filled with the phosphate buffer under a glass cover slip. The fluorescence associated with the carboxylate surface groups was then viewed by fluorescence microscopy using a 20 \times objective, a mercury lamp, a fluorescein filter set, and a CCD camera for detection. Since the PMMA intrinsically fluoresces prior to EDAC/aminofluorescein labeling, the average net intensity presented in this paper is the difference between the average measured intensity from the recorded fluorescence image and the average background fluorescence that was measured prior

to placing the sample in the EDAC/aminofluorescein solution. The fluorescence intensity for each channel was measured before and after labeling and at three separate locations along the length of each channel.

Microchannel Sealing Procedure. For the electroosmotic flow studies, the preformed microchannels were covered and thermally sealed with a similar, flat piece of PMMA, referred to as the "lid". Circular, 3-mm-diameter, holes in the lid provided access to the channels and served as fluid reservoirs. Prior to bonding, the lid and the channel were cleaned with a compressed nitrogen jet. The lid was then placed on top of the channel, and the two pieces were clamped together between microscope glass slides and bonded by heating in a circulating air oven at $103.0 \pm 0.5 \text{ }^\circ\text{C}$ for 12 min. It is important to keep the time and temperature as low as possible in the sealing process to avoid physical alteration of the microchannel surface.

Flow Image Acquisition. The system and procedure for uncaging the caged fluorescein and acquiring the corresponding flow images has been described in detail in a previous publication;¹⁵ however, a brief overview will be presented here. Uncaging of the fluorescein dye in the microchannels was performed using the output of a pulsed nitrogen laser (337 nm, pulse duration <4 ns, pulse energy 300 μJ) that was focused onto the channel through a 5 \times microscope objective. The angle of incidence of the laser pulse relative to the top surface of the lid was set to 55°, so that the "footprint" of the laser pulse at the plane of the microchannel was spread into a line 5 μm wide and 300 μm long. An important consideration in using this technique is that the materials used in the fabrication of the microchannels must be transparent at the wavelength of the uncaging pulse.

Fluorescence imaging of the uncaged dye was performed using a research fluorescence microscope equipped with a long working distance objective (10 \times for channels with 90° turn, 20 \times for straight channels), a mercury arc lamp, a fluorescein filter set, and a video camera (COHU, San Diego, CA). Digital images were acquired using Scion Image software and a Scion LG-3 frame grabber (Scion, Inc., Frederick, MD). The camera signal was interlaced, so that on each frame of acquired video, the odd-numbered and even-numbered horizontal lines represented distinct video fields. After capturing the images, the data were processed to separate the odd and even fields, providing a data rate of 60 images/s.

Measurement of Electroosmotic Flow. To image and measure the electroosmotic flow, the microchannels were filled with the caged dye solution. An equal amount (typically 50 μL) of solution was placed in each of the fluid reservoirs, and platinum electrodes were placed in contact with the solution in the reservoirs. The microchannel was placed beneath the fluorescence microscope as described in the previous section and aligned so that it was perpendicular to the line formed by the uncaging pulse. Sequences of images were acquired at several different applied voltages, beginning and ending with zero applied voltage to verify that the magnitude of the mean velocity resulting from pressure gradients along the channel was less than 10 $\mu\text{m/s}$. The current through the microchannel was determined by measuring the voltage drop across a 100-k Ω resistor (typically less than $1/1000$ the resistance of the microchannel) connected to the high-voltage supply in series with the microchannel.

(36) Hermanson, G. *Bioconjugate Techniques*; Academic Press: San Diego, CA, 1996; pp 172–173.

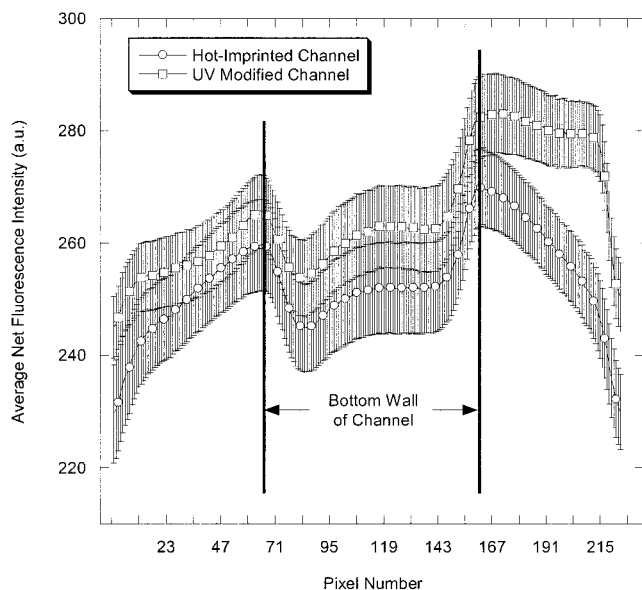


Figure 2. Average net fluorescence intensity profile of aminofluorescein labeled carboxylate groups on the surface of the nonmodified and UV-modified, hot-imprinted microchannel. Error bars represent the standard error of the mean.

Safety considerations: UV laser energy is dangerous and standard laboratory safety equipment should be used, including protective eyewear.

RESULTS AND DISCUSSION

Carboxylate Labeling of Microchannels. The EDAC/aminofluorescein labeling of surface carboxylate groups was conducted on hot-imprinted, straight channels and hot-imprinted, straight channels with a UV-modified surface. A total of four acrylic substrates were imprinted with three imprinted channels per substrate. Two of the four substrates were used for the UV modification studies. The average net fluorescence profiles related to the concentration of carboxylic acid groups and the standard errors of the mean of the measurements across the width of the channels are shown in Figure 2. From this figure, it can be seen that there is a statistical increase in the number of carboxylate groups present on the UV-modified wall compared to the nonmodified imprinted channel. The increase in the number of carboxylate groups due to UV subablation exposure is in agreement with previously published data²⁸ and results in an increased surface charge.

Caged Fluorescein Flow Studies. Straight Channels. Using the caged fluorescein dye, we have observed electroosmotic flow in a single, straight channel without a UV-modified surface at electric fields of 266, 532, and 718 V/cm and with a single, UV-modified surface at 244, 488, and 732 V/cm. The experiment was repeated twice at each applied field. The dimensions of the straight, trapezoidal-shaped channels are 73 μm wide at the top, 25 μm wide at the bottom, and 31 μm deep. A time series of images for electrokinetic flow in a nonmodified and a UV-modified, straight microchannel are shown in Figure 3a,b for applied fields of 532 and 488 V/cm, respectively. A comparison of panels a and b of Figure 3 clearly shows that there is an increase in the electroosmotic mobility, resulting from an increase in the surface charge, over the region of the microchannel that has been UV-

modified. This is in agreement with the carboxylate labeling study presented in Figure 2.

For the nonmodified, straight microchannel (Figure 3a), there is a small deviation from ideal plug flow with a slightly greater velocity in the middle of the channel than at the edges due to a nonuniform density of surface charges²⁸ and a nonuniform temperature profile.³⁷ Also, for the experiments in the UV-modified, straight microchannel (Figure 3b), there appears to be some tailing of the caged dye fluorescence at the edges of the UV-modified surface. This tailing is due to a nonuniform charge on the wall, resulting from the fact that the width of the UV pulse was slightly less than the width of the channel wall. The beam-defining aperture and corresponding magnification resulted in a 15.5- μm -diameter UV exposure on the surface of the PMMA. The projected width of the side wall is 22.5 μm ; thus, there will be non-UV-modified regions on either side of the exposure area, if the beam were perfectly centered over the side wall. This unexposed region has a lower surface charge than the UV-modified region, as shown in Figure 2, and results in the decrease in the electrokinetic flow, and the tailing effect, as shown in the Figure 3b.

Increase in Electroosmotic Velocity. To investigate the increase in the electroosmotic mobility between the UV-modified surface and the opposing nonmodified side wall of the straight channel shown in Figure 3b, the average velocities, u_{tot} , of the uncaged dye within 13 μm from the sides of the channel were determined. This was done by calculating the position of the center of the sample as a function of time within this region. The center of the uncaged dye was calculated numerically and is defined as the point at which half the total integrated intensity was equally distributed to the left and right.

Since the uncaged fluorescein dye is charged, the measured velocity is equal to the sum of the electrophoretic and electroosmotic velocities. The electrophoretic mobility was calculated from the measured diffusion coefficient,¹⁵ $D_0 = (4.6 \pm 0.2) \times 10^{-6}$ cm^2/s , using the Nernst–Einstein relation to give $\mu_{\text{EP}}^0 = (-3.4 \pm 0.2) \times 10^{-4}$ $\text{cm}^2/\text{V}\cdot\text{s}$ for small electric fields. At higher electric field, μ_{EP} increases due to Joule heating since, like the conductivity, it is proportional to $1/\eta$, where η is the buffer viscosity. Consequently, the electrophoretic velocity can be calculated as $u_{\text{EP}} = \mu_{\text{EP}}^0 E(R_0/R)$, where E is the electric field, R is the microchannel resistance, and R_0 is the resistance extrapolated to zero field. The electroosmotic mobility is then given by $\mu_{\text{EO}} = (u_{\text{tot}} - u_{\text{EP}})/E$. The average ratio of the electroosmotic mobilities of the UV-modified side wall, $\mu_{\text{EO}}^{\text{UVMod}}$, and the opposing nonmodified side wall, $\mu_{\text{EO}}^{\text{NoMod}}$, for the images shown in Figure 3b is $\mu_{\text{EO}}^{\text{UVMod}}/\mu_{\text{EO}}^{\text{NoMod}} = 1.0423$. This corresponds to an average increase in the electroosmotic flow of 4% for the modified versus the nonmodified wall. The standard error of the mean of the ratio of electroosmotic mobilities is 9.6×10^{-3} . Similar calculations were done for the images shown in Figure 3a, and the average ratio of the electroosmotic mobilities between the two opposing side walls was $\mu_{\text{EO}}^{\text{SideWall1}}/\mu_{\text{EO}}^{\text{SideWall2}} = 0.9965$, with a standard error of the mean equal to 0.7×10^{-3} . A two-sample *t*-test assuming nonequal variances for the ratio of electroosmotic mobilities indicates that there is greater than 95% probability that the two mobility ratios are statistically different.

(37) Ross, D.; Locascio, L. E. *Anal. Chem.* In press.

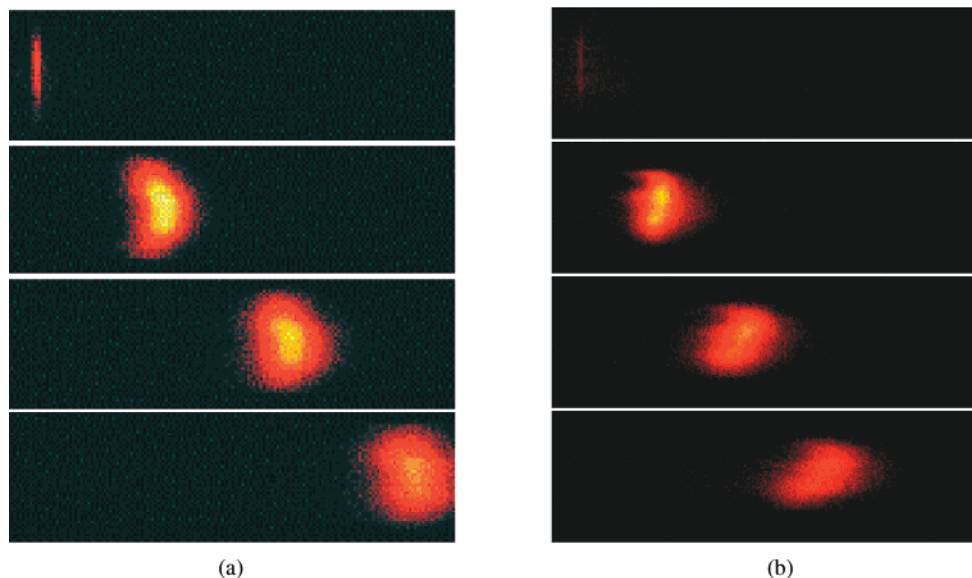


Figure 3. Top view of electrokinetic flow profiles as observed by fluorescence microscopy for (a) a nonmodified and (b) a UV-modified, hot-imprinted microchannel with an applied electric field of (a) 532 and (b) 488 V/cm, respectively. Note that the flow profile at later times is skewed in (b) compared to (a) due to the increased electroosmotic flowrate over the UV-modified surface. The time step between images was 50 ms.

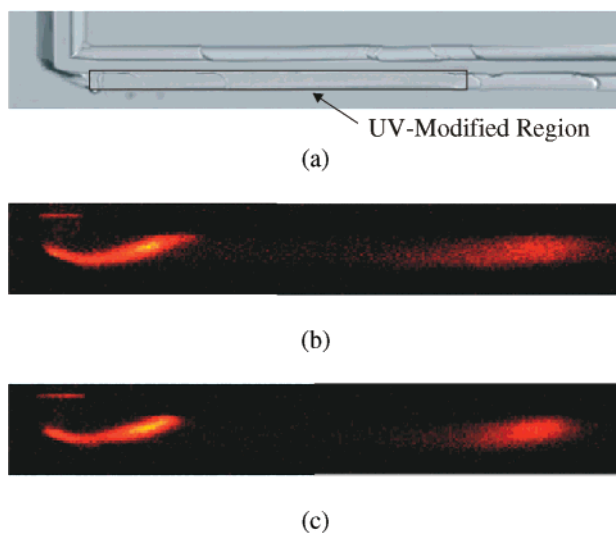


Figure 4. (a) Top view, white light image of a UV-modified, 90°-turn microchannel. Top view, electroosmotic flow profiles as observed by fluorescence microscopy in (b) a nonmodified and (c) a UV-modified, 90°-turn microchannel, and an applied electric field of (b) 454 and (c) 476 V/cm. The time step between peaks was (b) 0, 83, and 417 ms and (c) 0, 67, and 333 ms. Note the reduction in band broadening for the UV-modified turn at later times.

The relationship between the electroosmotic mobility and the zeta potential, ζ , is given by Smoluchowski's equation $\mu_{\text{EO}} = -\epsilon\epsilon_0\zeta/\eta$, where ϵ is the dielectric constant of the buffer and ϵ_0 is the permittivity of free space. A ζ of -84.3 mV is obtained for a nonmodified wall by assuming the viscosity of water at 298 K, a dielectric constant of 78.5, and an average electroosmotic mobility of 6.5×10^{-4} cm²/V·s from measurements taken over the range of 50–750 V/cm. A 4% increase in the electroosmotic mobility for the UV-modified wall would then translate into a ζ of -87.9 mV. However, when the 4% increase in the electroosmotic mobility was being determined, it was not possible to account for the Taylor

dispersions of the uncaged dye that results from any nonequal surface charge densities between walls of the channel. This dispersion becomes especially important when the mobility in the region between the UV-modified wall and the lid is being calculated. Since the peak dispersions will act to retard the calculated increase in the electroosmotic mobility for the UV-modified surface, and therefore the ζ , the actual increase in ζ is probably greater than 4%. For a further discussion of the effects of differing charge densities between the walls of a microchannel on the electroosmotic flow, the reader is referred to Bianchi et al.³⁸

Caged Fluorescein Flow Studies. 90°-Turn Channels.

Using the caged fluorescein dye, we have also observed the electroosmotic flow for various applied fields in a single hot-imprinted channel and a single hot-imprinted channel with a UV-modified surface, for channels with a 90° turn. The experiment was repeated twice at each applied field. The dimensions of the trapezoidal-shaped channels are 57.5 μm wide at the top, 36.2 μm wide at the bottom, and 26.0 μm deep prior to the turn and are 52.0 μm wide at the top, 29.0 μm wide at the bottom, and 26.0 μm deep after the turn. For this experiment, the width of the side walls was more closely matched with the width of the UV excimer exposure area to minimize the tailing effect previously discussed for Figure 3b. A white light image of a UV-modified, 90°-turn microchannel is shown in Figure 4a. Also, a time series of images for electrokinetic flow in a nonmodified, 90°-turn microchannel and a time series of images for flow in a UV-modified, 90°-turn microchannel are shown in panels b and c of Figure 4, respectively. The applied electric fields were 454 and 476 V/cm for the experiments in the nonmodified and UV-modified channel, respectively. Figure 4c clearly shows that there is a decrease in the tailing of the uncaged fluorescein band as it exits the UV-modified region compared to the band located at a similar position within

(38) Bianchi, F.; Wagner, F.; Hoffmann, P.; Girault, H. H. *Anal. Chem.* **2001**, *73*, 829–836.

the nonmodified channel, Figure 4b. It should be noted that while the electric fields differed slightly between the two experiments, a direct comparison of band broadening can still be made when comparing plate heights, as discussed below.

Reduction of Band Broadening. The plate height, $H \equiv 2D_{\text{eff}}/u_{\text{EO}}$, for nonmodified and UV-modified, 90°-turn channels as well as nonmodified, straight channels was calculated to investigate the reduction in band broadening for electroosmotic flow around UV-modified, 90°-turn channels. The quantities D_{eff} and u_{EO} are the effective diffusion coefficient and the electroosmotic velocity (as calculated above), respectively. The effective diffusion coefficient incorporates dispersion of the caged dye due to diffusion, Taylor dispersion, and Joule heating, and it is calculated by measuring the width of the uncaged dye as a function of time. The width of the dye peaks was measured from the fit to the data, which was a Gaussian peak shape for the dye in the straight channel and in the 90°-turn channel prior to the turn. As the dye exited the turn, the data was fit to a summation of two Gaussian peaks because this shape was able to best fit the data and to capture the tailing induced by flow around the turn. The width, w , of the fluorescence peak was defined as the distance between the right and left edges of the curve fits. The left edge was defined as the point at which 10% of the integrated area was to the left and 90% was to the right, and the right edge as the point at which 90% was to the left and 10% to the right. Similarly, the center of the peak was defined as the point at which half the total integrated intensity was to the left and half was to the right. The effective diffusion constant can then be determined by fitting the data to the form

$$w^2 = 13.139D_{\text{eff}}(t - t_0) \quad (1)$$

where t is the time and the factor of 13.139 gives the correct relation between w as defined above and the diffusion constant for a fully integrated Gaussian peak shape. To properly analyze the reduction in band broadening in the UV-modified turn, the two peaks that were chosen to determine the effective diffusion coefficient were the first peak after the uncaging pulse and the first peak whose midpoint and half peak width were located beyond the modified region. For the nonmodified, 90°-turn channel, peaks at similar locations were analyzed.

The plot of plate height versus electroosmotic velocity for the various microchannels is shown in Figure 5. The solid line is the limiting case of $2D_0/u_{\text{EO}}$, and the dashed line shows the effect of uniform Joule heating. From this figure it can be seen that the use of UV modification results in a 40% reduction, on average, in the plate height compared to flow around a nonmodified, 90° turn.

CONCLUSIONS

We have shown that a pulsed UV excimer laser can modify the surface chemistry and surface charge of a previously imprinted microchannel in PMMA, without changing the physical dimensions of the channel. Fluorescence results from carboxylate labeling experiments confirm a statistical increase in the number

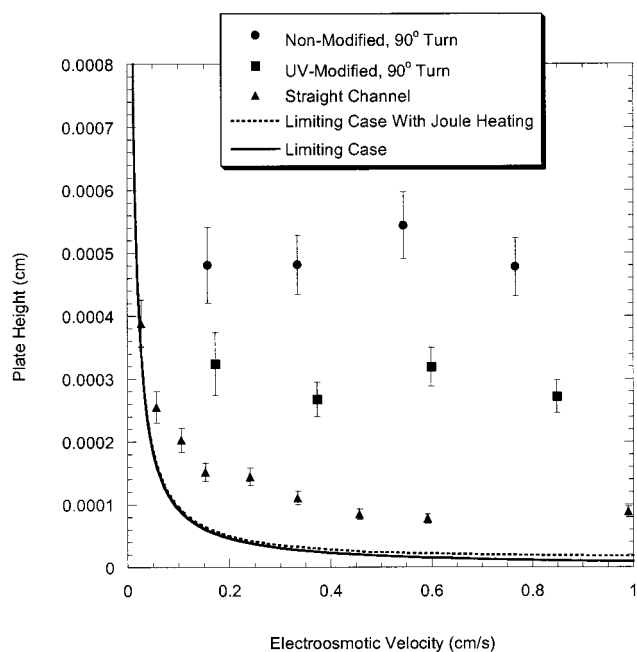


Figure 5. Plate height as a function of electroosmotic velocity for flow around nonmodified and UV-modified, 90°-turn microchannels compared to flow in straight microchannels. The solid line is the limiting case of $H = 2D_0/u_{\text{EO}}$. The dashed line shows the expected effect of increased diffusion due to uniform Joule heating.

of carboxylate groups on UV-exposed surfaces, which leads to an increase in the surface charge, compared to nonmodified surfaces. The increase in the surface charge is confirmed by the electrokinetic flow studies with the caged fluorescein dye. Results show that the electroosmotic mobility increases by an average of 4% with UV-modified surfaces compared to nonmodified surfaces without changing the channel morphology. Furthermore, it has been shown that UV modification can be used to reduce the band-broadening effects of electroosmotic flow around turns. Results show that a 40% reduction in the plate height can be achieved by modifying the outer wall of the turn with subablation level pulses. These results suggest that UV exposure can spatially modify surface charges to create desired electrokinetic flow profiles, without the use of wall coatings or the need to change the channel dimensions.

ACKNOWLEDGMENT

The authors acknowledge the financial support of the NRC/NIST Postdoctoral Research Program. Certain commercial equipment, instruments, or materials are identified in this report to specify adequately the experimental procedure. Such identification does not imply recommendation or endorsement by the National Institute of Standards and Technology, nor does it imply that the materials or equipment identified are necessarily the best available for the purpose.

Received for review March 5, 2001. Accepted May 18, 2001.

AC010269G